Electronic Supplementary Material (ESI) for Physical Chemistry Chemical Physics

Supporting information

Speciation dynamics of metals in dispersion of nanoparticles with discrete distribution of charged binding sites.

Pavel D. Polyakov,[1,2] Jérôme F. L. Duval[1,2*]

[1] Université de Lorraine, Laboratoire Interdisciplinaire des Environnements Continentaux (LIEC), UMR 7360, 15 avenue du Charmois, Vandœuvre-lès-Nancy, F-54501, France.

[2] CNRS, Laboratoire Interdisciplinaire des Environnements Continentaux (LIEC), UMR 7360, 15 avenue du Charmois, Vandœuvre-lès-Nancy, F-54501, France.

* Corresponding author:

Jérôme F. L. Duval: jerome.duval@univ-lorraine.fr

Tel: 00 33 3 83 59 62 63. Fax: 00 33 3 83 59 62 55.

I. Details of the analytical derivation of k_a^{os} for a single metal-binding site (eqn (21), Figure 2).

Equation (17) in the main text may be rewritten in the form

$$k_1^{os} = (2\pi r_p D_M N_a) f_{el}(\bar{a}) \int_{\varphi-\gamma}^{\varphi+\gamma} F(\alpha,\sigma)\mathrm{d}\alpha \qquad \text{(S1)}$$

where we have introduced the function *F* defined by

$$F(\alpha,\sigma) = \left[\bar{s}_{os}{}^2 + \bar{r}_0\bar{s}_{os}\cos(\alpha-\varphi)\right]\left[\bar{r}_0\cos(\varphi)+\bar{s}_{os}\cos(\alpha)\right]/\bar{r}^3 \qquad \text{(S2)}$$

and we developed eqn (17) using the relationships $\cos(\beta) = \left(\bar{r}^2 + \bar{s}_{os}{}^2 - \bar{r}_0^2\right)/\left(2\bar{r}\times\bar{s}_{os}\right)$ and $\bar{r} = (\bar{r}_0^2 + \bar{s}_{os}{}^2 + 2\bar{r}_0\bar{s}_{os}\cos(\alpha-\varphi))^{1/2}$ that are obtained upon inspection of Figure 2. $F(\alpha,\sigma)$ can be Taylor-expanded in terms of $\sigma = \bar{s}_{os}/\bar{r}_0$ for $\sigma << 1$. Under such condition, the quantity $1/\bar{r}^3$ in eqn (S2) is

$$\left[\bar{r}_0^2 + \bar{s}_{os}{}^2 + 2\bar{r}_0\bar{s}_{os}\cos(\alpha-\varphi)\right]^{-3/2} \approx \frac{1}{\bar{r}_0^3}\left\{1 - 3\sigma\cos(\alpha-\varphi) + \frac{\sigma^2}{2}(15\cos^2(\alpha-\varphi)-3)\right\}. \qquad \text{(S3)}$$

After combining eqns (S2) and (S3) and retaining the only terms of order $\sigma, \sigma^2, \sigma^3$, eqn (S2) reads as

$$F(\alpha,\sigma) \approx \sigma f_1(\alpha) + \sigma^2 f_2(\alpha) + \sigma^3 f_3(\alpha) \tag{S4}$$

where

$$f_1(\alpha) = \cos(\varphi)\cos(\alpha-\varphi) \tag{S5}$$

$$f_2(\alpha) = \cos(\varphi)\left[1-3\cos^2(\alpha-\varphi)\right] + \cos(\alpha-\varphi)\cos(\alpha) \tag{S6}$$

$$\begin{aligned} f_3(\alpha) = {} & -3\cos(\varphi)\cos(\alpha-\varphi) + \cos(\varphi)\cos(\alpha-\varphi)\left[(15/2)\cos^2(\alpha-\varphi) - (3/2)\right] + \ldots \\ & + \cos(\alpha) - 3\cos^2(\alpha-\varphi)\cos(\alpha) \end{aligned} \tag{S7}$$

After evaluation of the integral in eqn (S1) with $F(\alpha,\sigma)$ given by eqns (S4)-(S7), we obtain

$$k_1^{os} = k_{a,p}(a/r_p)\cos(\varphi)\left\{\sigma\sin(\gamma) + \sigma^2(-\frac{1}{2})\sin(2\gamma) + \sigma^3\left(\frac{3}{8}\sin(3\gamma) - \frac{1}{8}\sin(\gamma)\right)\right\} \tag{S8}$$

From Figure 2, it is straightforward to show that

$$\gamma = \pi/2 + d\varphi/2 = \pi/2 + \arcsin(\sigma). \tag{S9}$$

With help of trivial trigonometry, we further have for $\sigma << 1$

$$\sin(\gamma) = \cos(\arcsin(\sigma)) = \sqrt{1-\sigma^2} \approx 1-\sigma^2/2 \tag{S10}$$

$$\sin(2\gamma) = -\sin(2\arcsin(\sigma)) = -2\sigma\sqrt{1-\sigma^2} \approx \sigma^3 - 2\sigma \tag{S11}$$

$$\sin(3\gamma) = -\cos(3\arcsin(\sigma)) = -\sqrt{1-\sigma^2}(1-4\sigma^2) \approx \frac{9\sigma^2}{2} - 1 \tag{S12}$$

Combining eqns (S10)-(S12) and eqn (S8), we finally obtain

$$k_1^{os} = k_{a,p}(\bar{a})\cos(\varphi)\left\{\sigma + O(\sigma^4)\right\}, \tag{S13}$$

which is eqn (18) given in the main text. A successful comparison between results obtained from eqn (S13) and those derived numerically following the approach detailed in the main text, is given in Figure S1.

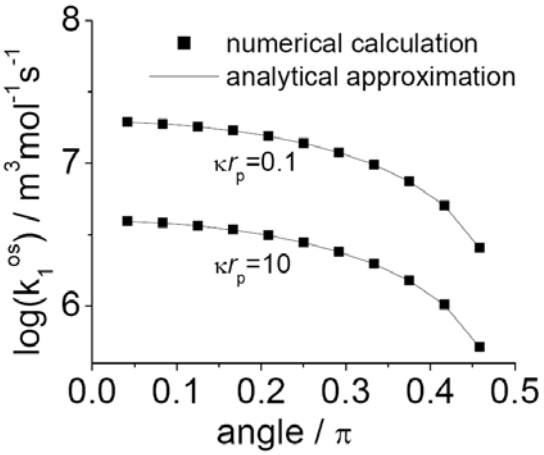

Figure S1. Dependence of k_a^{os} on the polar angle φ in the hard particle limit ($a = 0.95 r_p$) for two values of electrolyte concentrations ($\kappa r_p = 10$, $\kappa r_p = 0.1$ with $r_p = 20$ nm) and a single charged metal-binding site located at $(\overline{r}_0 = r_p - s_{os}, \varphi)$ (see nomenclature in Figure 2), $D = 10^{-9}$ m^2 s^{-1}. Numerical calculation corresponds to evaluation from eqn (3) and analytical results pertain to prediction from eqn (18), with the electrostatic potential derived from eqns (20),(21) (smeared-out electrostatics) in both cases. The total charge of the soft shell layer is $Q = 100e$. Under the conditions of Figure S1, the parameter $\sigma = 2.5\times10^{-3}$ involved in eqn (18) is << 1, which justifies the Taylor decomposition of k_a^{os} with respect to σ.

II. Derivation of the potential distribution for point-like charges in a porous particle under Debye-Hückel condition.

We adopt the spherical coordinate system ($|\boldsymbol{r}|, \theta, \varphi$) with the origin at the center of a porous particle. The local charge density of the point-like charges distributed throughout the particle may be written in terms of Dirac delta functions according to

$$\rho_{fix}^{ds}(\boldsymbol{r}) = e\sum_{i=1}^{N_s}\delta(\boldsymbol{r} - \boldsymbol{r_i}) \tag{S14}$$

where $\boldsymbol{r_i}$ is the position of the charge i and the delta function is further defined as

$$\delta(\boldsymbol{r} - \boldsymbol{r_i}) = \frac{1}{V_p}\frac{1}{|\overline{\boldsymbol{r}}|^2}\delta(|\overline{\boldsymbol{r}}| - |\overline{\boldsymbol{r_i}}|)\delta(\cos(\theta) - \cos(\theta_i))\delta(\varphi - \varphi_i) \tag{S15}$$

with V_p the particle volume. Within the framework of the Debye Hückel approximation, eqn (20) in the main text reads in spherical coordinates

$$\Delta y(|\overline{\boldsymbol{r}}|, \theta, \varphi) - (\kappa r_p)^2 y(|\overline{\boldsymbol{r}}|, \theta, \varphi) = -(\kappa r_p)^2 \overline{\rho}_{fix}(|\overline{\boldsymbol{r}}|, \theta, \varphi) \qquad \text{with} \tag{S16}$$

$$\overline{\rho}_{fix}(|\overline{\boldsymbol{r}}|, \theta, \varphi) = \frac{e}{2zFc^* V_p}\sum_{i=1}^{N_s}\frac{1}{|\overline{\boldsymbol{r}}|^2}\delta(|\overline{\boldsymbol{r}}| - |\overline{\boldsymbol{r_i}}|)\delta(\cos(\theta) - \cos(\theta_i))\delta(\varphi - \varphi_i) \tag{S17}$$

The solution of eqn (S16) is expressed by the well-known Green function for the Helmholtz equation, *i.e.*

$$y(|\overline{\boldsymbol{r}}|, \theta, \varphi) = \frac{e}{2zFc^* V_p}\sum_{i=1}^{N_s}\frac{\exp\{-\kappa r_p |\overline{\boldsymbol{r}} - \overline{\boldsymbol{r_i}}|\}}{4\pi|\overline{\boldsymbol{r}} - \overline{\boldsymbol{r_i}}|} \tag{S18}$$

In order to test the validity of our numerical scheme, we considered the situation where seven point-like charges e were randomly distributed from the center of a soft particle to its outer surface along the radial direction. In order to avoid numerical instabilities, the electrostatic potential distributions were evaluated up to small sphere of radius $\sigma \to 0$ that enclosed each point-like charge within the particle. Figure S2 shows a perfect agreement between the analytical results obtained from eqn (S18) and the results obtained from our

numerical solution of linearized Poisson-Boltzmann equation in the extremes of thin and thick electric double layers as compared to particle radius ($\kappa r_p = 10$, $\kappa r_p = 0.1$ with $r_p = 20$nm) (eqns (20),(22)).

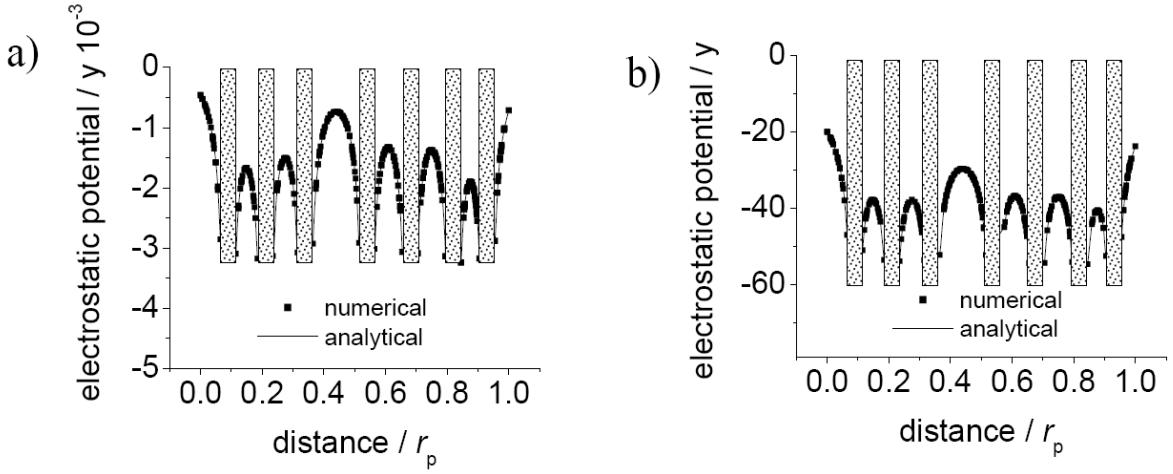

Figure S2. Electrostatic potential profiles as the function of the radial distance from the porous particle centre for seven randomly distributed point-like charges e located at the center of the ligands. Comparison between numerical results (eqns (20),(22) with $s_{os} \to 0$) and the analytical expression given by eqn (S18). (a) $\kappa r_p = 10$, (b) $\kappa r_p = 0.1$. $r_p = 20$nm. Vertical bars indicate the positions of the ligands.

III. Examples of statistical distribution of site-to-site distances in the soft particle limit for uniform and non-uniform site distributions.

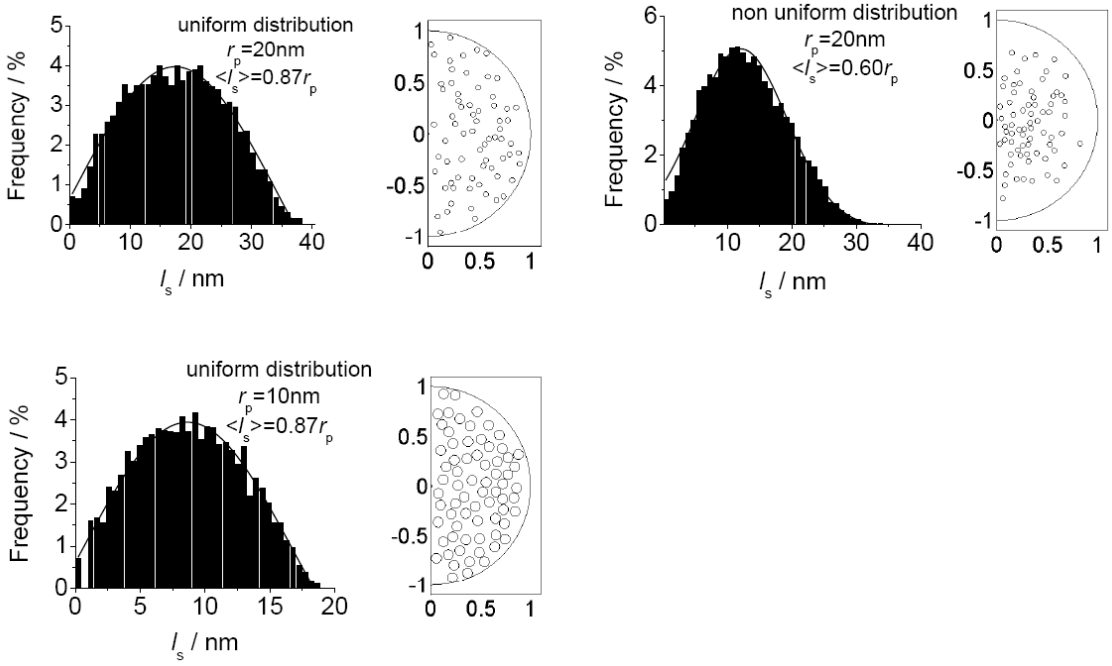

Figure S3. Statistical distribution of the site-to-site distance in the soft particle limit $a = 0.01 r_{\mathrm{p}}$ ($N_{\mathrm{s}} = 70$). (a) Uniform distribution, $r_{\mathrm{p}} = 20\mathrm{nm}$, (b) Non-uniform distribution, $r_{\mathrm{p}} = 20\mathrm{nm}$, (c) uniform distribution, $r_{\mathrm{p}} = 10\mathrm{nm}$. Uniform and non-uniform site distributions correspond here to the density probability functions $\Phi\left(\bar{x},\bar{z}\right) = 1/\pi$ and $\Phi\left(\bar{x},\bar{z}\right) = 6\left(1-\sqrt{\bar{x}^2+\bar{z}^2}\right)^2/\pi$, respectively. For each case, we give the corresponding spatial distribution of ligands within the porous particle.